Direct Observation of Polymer Network Structure in Macroporous *N*-Isopropylacrylamide Gel by Raman Microscopy

Rainer Appel, Wei Xu, and T. W. Zerda

Department of Physics, Texas Christian University, Fort Worth, Texas 76129

Zhibing Hu*

Department of Physics, University of North Texas, Denton, Texas 76203

Received August 20, 1997; Revised Manuscript Received January 20, 1998

ABSTRACT: The Raman microscopy technique is used to characterize the temperature-induced evolution of the pore structures of a macroporous *N*-isopropylacrylamide (NIPA). The gel is synthesized using a suspension of 45 wt % toluene and 55 wt % pregel NIPA solution. The intensity of the band due to the CH_2 bending vibration, centered at 1445 cm^{-1}, is used to monitor the distribution of the polymer chain density in the lateral plane. It is found that the macroporous gel consists of water-rich areas, which can be interpreted as the pores, and polymer-rich areas. At room temperature, the average sizes of the pores and the width of polymer-rich areas are 75 μm and 20 μm, respectively. Both the pores and their surrounding polymer-rich areas have random geometry, as demonstrated by the Raman microimaging. With increased temperature the size of the pores decreases. This process is accompanied by a narrowing of the polymer-rich areas. At higher temperatures polymer chains bunch together and this process accelerates rapidly near the volume phase transition temperature (34 °C). Above 36 °C, the pore sizes become too small to be resolved using Raman microscopy.

Introduction

Characterization of the microstructure of polymer gels can lead to a better understanding of macroscopic properties such as texture, permeability, and elasticity.[1] Precise determination of pore structures in a hydrogel is particularly important, but direct measurements are difficult. Conventional electron microscope techniques have been used in the past but results obtained, although informative and important, are not completely reliable because the inherent pore structure cannot be preserved during the sample preparation. For example, the freeze-dry method used by some researchers often leads to the collapse of the pore structure due to ice formation and/or volatile evaporation in a vacuum.[2] Another technique used to determine the pore structure, the atomic force microscope, can be applied to a gel in water, but the results are limited only to the surface analysis.[3]

The lack of direct and nonintrusive measurements of pore structures in hydrogels was the motivation for the present study. Here, we propose and demonstrate that Raman microscopy is a powerful tool to study the macroporous structure of polymer gels. Raman microscopy has been utilized to provide information about molecular vibrations from small samples.[4,5] In the lateral plane, perpendicular to the optical axis, spatial resolution better than 1 μm has been achieved by focusing the beam on the substrate through a 100× objective.[6] A two-dimensional molecular map of the sample can be acquired by moving the sample step-by-step along one direction and then repeating the measurements along a parallel line displaced by a small step, usually greater than or equal to the beam diameter. The construction of three-dimensional images requires displacement of the sample along the optical axis. However, the spatial resolution along the vertical direction is usually not as good as in the lateral direction but can be improved by placing a pinhole in the back focal plane of the microscope. Confocal Raman microscopy has been used to study the distribution of components inside various materials, such as binary mixtures of polymers,[6] composites,[7] biological tissues,[8] and others.

In this paper we discuss Raman spectra of the macroporous *N*-isopropylacrylamide (NIPA) gels and the temperature dependence of the two-dimensional distribution of the polymers chains within the gels. The NIPA gel is a member of the class of hydrogels that undergo the volume phase transition upon heating.[1] This transition takes place around 34 °C and is caused by hydrophobic interactions between NIPA polymer chains. A conventional, homogeneous NIPA gel has the network mesh size around 5 nm.[9] In contrast, the macroporous NIPA gel has pore sizes varying between 10 and 100 μm. This length scale is mostly suitable for investigation by Raman microimaging. Macroporous gels provide unique advantages such as fast kinetics, high throughput, immobilizing large biomolecules, and separation of large objects, like nucleic acids.[10,11] It is possible that the information obtained from Raman studies can help optimize the synthesis conditions to obtain a desired pore structure.

Experimental Section

The process of synthesis of macroporous NIPA gels was based on the suspension principle.[12,13] The first step was to form an oil-in-water suspension, wherein the water phase (100 mL) contains a water-soluble NIPA monomer (7.8 g) and a cross-linking agent (133 mg of methylenebis(acrylamide), 133 mg). The oil phase is a volatile toluene (45 wt %) having a boiling point of 110 °C. A dispersing agent (0.284 g of poly(vinyl alcohol)) capable of suspending the oil phase was added. The NIPA solution was polymerized by adding both an initiator (ammonium persulfate (40 mg)) and an accelerator (tetramethylethylenediamine (240 μL)). The resultant NIPA was then dried at a temperature above the boiling point of toluene. As toluene volatilized, it

* To whom the correspondence should be addressed.

S0024-9297(97)01260-6 CCC: $15.00
Published on Web 07/03/1998

expanded and blew holes in the gel. The samples were reswollen in water and thoroughly washed.

A gel in the shape of a cylinder was placed in a glass vial filled with deionized and distilled water. The vial was secured inside a heating jacket and the temperature was controlled with precision better than 0.1 °C. The heating jacket was mounted onto the $x-y-z$ positioning stage. The vial was covered with a microscope slide 0.1 mm thick. The position of the gel inside the vial was adjusted in the vertical direction so it gently pressed onto the microscope slide. This arrangement assured us that the surface of the gel was flat and parallel to the horizontal surface of the $x-y-z$ positioning stage.

Raman spectra were obtained by illuminating the sample with an argon laser operating at the wavelength of 488 nm. The laser beam was focused by a 100× objective of a confocal microscope, Olympus BH2, and the waist of the laser beam on the flat surface of a silicon wafer was 0.5 μm in diameter. The scattered light was collected by the same objective and the spectral analysis was done using an axial transmissive spectrograph (Kaiser Optical Systems, HoloSpec) equipped with a Princeton Instrument CCD camera. Raman spectra of the NIPA gels, in the frequency range between 200 and 1700 cm^{-1}, were obtained using a 10 s integration time. The spectra were analyzed using spectroscopic software, GRAM 32.

Spatial resolution of Raman measurements is determined by the size of the laser beam, the size of the pinhole in the back focal plane, and the precision of the $x-y-z$ table. The computer-controlled $x-y-z$ positioning stage (Oriel, Encoder Mike) was capable of advancing the specimen in either direction in steps as small as 0.1 μm. However, the measured effects were much larger and only negligibly small changes in the polymer distribution were observed when the sample was displaced in those very small steps, and we selected a larger step of 2 μm. To determine the spatial resolution of our instrument, we used Raman microimaging to measure the size of latex spheres of precisely defined diameters, 25.7 μm, supplied by E. Fullam. The diameters of the spheres were confirmed by independent measurements using an optical microscope. Two pinholes of diameters 500 and 100 μm were used. For those pinholes, the resolutions in the vertical direction were 10 and 4 μm, respectively. However, for both pinholes, the lateral resolution was better than 4 μm and limited by the size of the step used in advancing the specimen. It is seen that the smaller pinhole gives a better vertical resolution; however, the signal-to-noise ratio was smaller for the small pinhole and most of the results presented in this paper were obtained using the 500 μm pinhole in the back focal plane. The larger pinhole allowed us to reduce the exposure time and operate the laser at relatively low power, 0.4 W.

To ensure that the selection of the pinhole did not affect the conclusions of this study, we scanned selected samples of the macroporous NIPA gel using pinholes of both sizes and found that all results, including numerical data, were identical.

Experiments were conducted at the following temperatures: 22.0, 26.2, 28.2, 29.7, 31.5, 32.3, 33.1, 33.9, 34.0, and 36.2 °C. Experiments were run 30 min after the equilibrium had been reached. The temperature was stable within 0.1 °C. The average scanning distance was 0.5 mm, but at the room temperature and at 34 °C we scanned the distances exceeding 3 mm. We obtained spectra of different samples, in each case the results were similar.

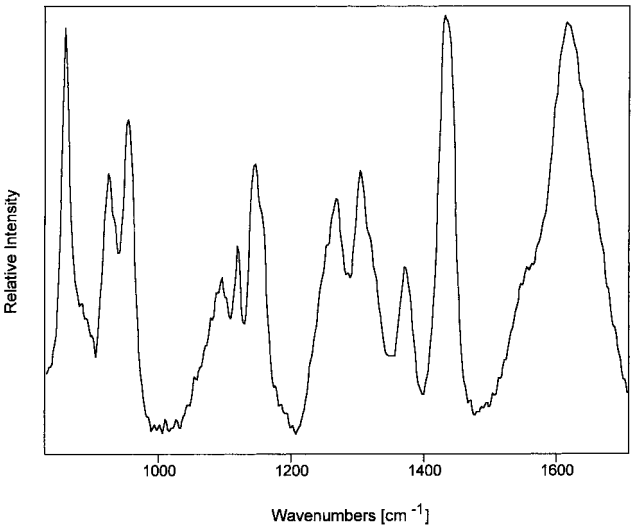

Figure 1. Raman spectrum of the NIPA gel at 22 °C. Spectral resolution is 1.5 cm^{-1}.

Results and Discussion

In Figure 1 we depict a typical Raman spectrum of a NIPA gel in the frequency range between 800 and 1700 cm^{-1}. The broad structure between 1040 and 1100 cm^{-1} and the sharp peak at 1125 cm^{-1} are assigned to various C−C skeletal stretching modes. The amide C−N stretch overlaps with the C−H deformation bands, resulting in a doublet with centers at 1279 and 1318 cm^{-1}. The CH_3 bending mode is observed at about 1380 cm^{-1}. The amide II mode, which is mainly due to the N−H vibration, is observed at 1560 cm^{-1} as a small shoulder of a broad band centered at 1620 cm^{-1}. The latter band is mainly due to the C═O vibrations, often referred to as the amide I band. The detailed analysis of this band, however, is obscured by the contribution due to the amide II band and the presence of water in the system. The broad peak of water overlaps with this band, making data analysis difficult.

We assumed that the intensity of the band due to the CH_2 bending vibration, centered at 1445 cm^{-1}, was proportional to the concentration of the polymer inside the focus of the laser beam. This band was selected because it is well isolated from other bands and the background can be precisely determined. Thus, the intensity of the band can be easily calculated. In Figure 2 we display the concentration of the polymer obtained from the 1445 cm^{-1} band intensity as it changes along the x-axis. As expected, it is seen that the polymer concentrates in regions that are separated by water. At 22 °C, the average thickness of the region of high concentration is about 20 μm, as shown in Figure 2A. These regions represent the polymer matrix separating adjacent pores. At 22 °C the average distance between the centers of the chain-rich areas is 75 μm. These values, which were obtained by scanning different gels in various directions over the total distance of 3 mm, refer to the pore/mesh parameters not the dimensions of individual polymer chains.

Due to a hydrophobic interaction among NIPA polymer chains, the NIPA gel shrinks upon heating. As a result, both the pore size and the width of the polymer-rich areas decrease, as shown in Figure 2B. It is interesting to note that starting at 32 °C the polymer

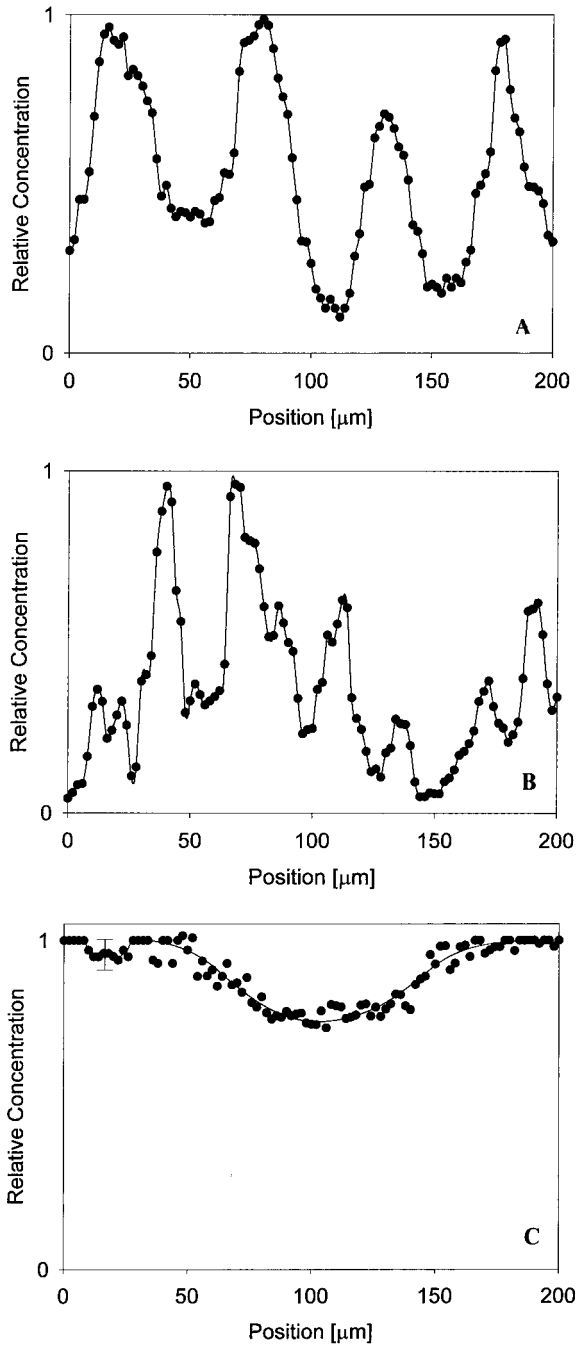

Figure 2. Variation of the polymer concentration along one direction within the gel. The concentration was calculated from the 1445 cm^{-1} Raman band intensity. The lines are drawn through the data points to guide the eye. The minima represent areas of higher water concentration. (A) $T = 22$ °C, (B) $T = 33.1$ °C, (C) $T = 34.0$ °C. The error bar shown in part C is a typical error for all the data points.

chains appear to bunch together and entanglements involving two and three bundles can be observed. The thickness of the bundles appears to become narrower with increasing temperature.

When the temperature is above the volume phase transition temperature, $T_c = 33.6$ °C, the gel collapses. It is impossible to distinguish individual pores; compare Figure 2C. The shallow dip at the central part of this figure is a typical observation, which also appeared in other scans recorded at this temperature. It represents the section of reduced polymer concentration. A further increase of the temperature results in the structure becoming increasingly more and more homogeneous, and above 36 °C the polymer concentration is uniform across the sample. Those results are not shown because a perfectly straight and horizontal line represents them. The lack of internal structure in the concentration distribution at $T > T_c$ may be explained as follows. The collapse of the gel volume at $T > T_c$ causes drastic shrinkage of pore sizes in both lateral and vertical directions. Within the resolution of the instrument, the pore structure cannot be distinguished. When the gel volume collapses, a transparent NIPA gel becomes opaque. The opacity is due to the spinodal decomposition,[14,15] which occurs when the polymer network concentration decomposes into smaller domains with two different densities, one dilute and the other dense. These additional domain structures may further smear out the Raman spectra as the temperature is increased from below T_c to above T_c.

Scans were run at different depths ranging from just below the gel surface down to 200 μm below the surface. Due to absorption and nonresonant scattering, the intensity of Raman bands decreases with increasing depth, and only spectra recorded at the same vertical depth can be compared and used to compute the concentration of the polymer. For those horizontal runs, the results were similar to those depicted in Figure 2.

In Figure 3 we show the two-dimensional distribution of the polymer concentrations in the macroporous NIPA gel over the region 100 μm × 30 μm at room temperature. The scan lines were recorded every 2 μm. The *z*-axis represents the concentration of the polymer. From this figure, one can identify the connectivity of the pores. Connectivity of the pores plays a crucial role in fast kinetics of the gels. Water can enter or leave the gel through these interconnected pores by convection. The process is much faster than the diffusion process that dominates the conventional, homogeneous gels. This point has been demonstrated by immersing a conventional NIPA gel and a macroporous NIPA gel with the same dimensions (1 cm in diameter and 1.2 cm thickness at room temperature) into a 39 °C water bath. The macroporous gel shrinks 14 000 times faster than the conventional gel. As a result, the macroporous gel has potential applications in gel sensors and devices.[16]

From Raman spectra we have obtained the following pictures of the pore structures of a conventional homogeneous NIPA gel and a macroporous NIPA gel. For a conventional NIPA gel, its average network mesh size is on the order of about 5 nm[9] and polymer chains are uniformly distributed. In fact, the Raman intensity at 1445 cm^{-1} remained the same as the laser was scanned through a conventional NIPA gel. For macroporous NIPA gels, their internal structure consists of numerous interconnected pores with the size (λ) on the order of 75 μm. These pores are surrounded by a bundle of polymer chains with the width (d) of the wall on the order of 20 μm. It is the nonuniform distribution of polymer chains that causes the variation of the Raman intensity. As the temperature increases from room temperature, the volume of the macroporous NIPA gel shrinks due to the increase of hydrophobic interactions among NIPA chains. As a result, both λ and d decrease with temperature. When the sample completely collapses at around 34 °C, the pore structure of the NIPA gel can no longer be resolved by the Raman microscopy.

It is noted that the microstructure of the polymer gels has been previously studied by Matsuo et al. using the

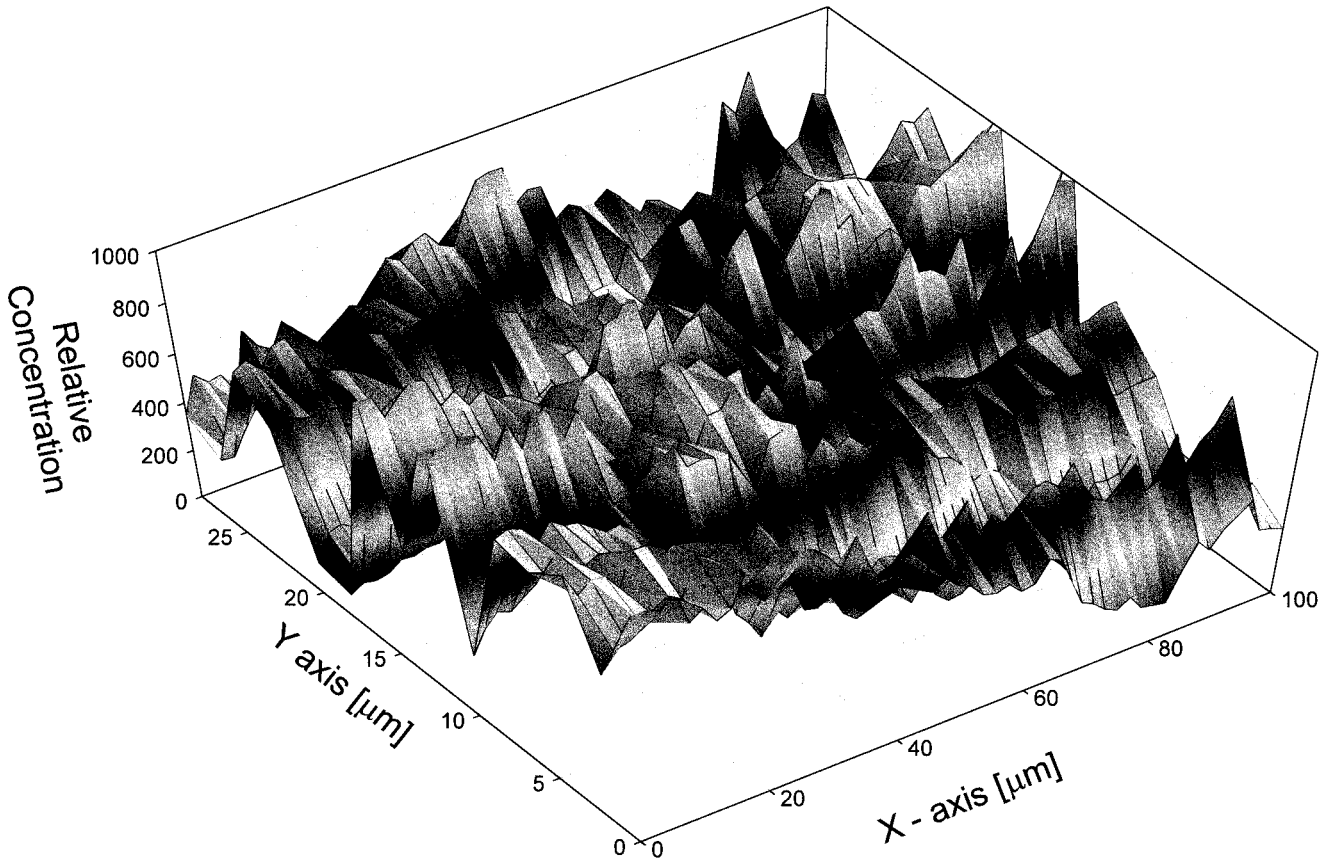

Figure 3. Distribution of the polymer network in the porous NIPA gel in water at 22 °C. For the clarity reason, only the even scan lines are shown.

light-scattering technique.[17] Concentration fluctuations in the polymer network give rise to intense light scattering. Matsuo et al. were able to differentiate between concentration fluctuations due to thermal fluctuation, domain formation on the onset of gelation, and domain formation due to microphase separation. Because of the different nature of the two experiments we were not able to identify the origins of density fluctuations, and in this paper we limit the discussion to the distribution of the polymer concentration. The polymer density concentration was obtained by assuming that the Raman band intensity is proportional to the density of scattering units, i.e., the density of molecular groups.

In conclusion, this study has shown that Raman microscopy is a very powerful tool for investigation of the pore structure of the macroporous NIPA gel. Distribution of polymer chains in the macroporous NIPA gel has been studied as a function of temperature using the Raman microimaging technique. At room temperature, the network is inhomogeneously connected and it is possible to distinguish areas of increased concentration of water, which can be interpreted as the pores. The pores have random geometry and the average size of the pore is 75 μm. With increased temperature the size of the pores decreases. This process is accompanied by the narrowing of chain bundles representing the walls separating adjacent pores. At higher temperatures chains bunch together; this process accelerates rapidly above 33 °C, and at 34 °C it is impossible to distinguish individual pores. The pore structure disappears completely above 36 °C.

Acknowledgment. Acknowledgment is made to the donors of the Petroleum Research Fund, administered by the American Chemical Society, and to the U.S. Army Research Office under Grant No. DAAG 55-98-1-0175 for support of this research. We thank Y. Li and Y. Chen for their help for sample preparation.

References and Notes

(1) Tanaka, T. ACS Symposium Series, No. 480; Harlard, O. S., Prud'homme, R. K., Eds.; American Chemical Society: Washington, DC, 1992, p 1. Li, L.; Tanaka, T. *Annu. Rev. Mater. Sci.* **1992**, *22*, 243. Shibayama, M.; Tanaka, T. *Adv. Polym. Sci.* **1993**, *109*, 1.
(2) Park, T. G.; Hoffman, A. S. *Biotechnol. Prog.* **1994**, *10*, 32.
(3) Suzuki, A.; Yamazaki, M.; Kobiki, Y. *J. Chem. Phys.* **1996**, *104*, 1751.
(4) Barbillat, J.; Dhamelincourt, P.; Delhaye, M.; Da Silva, E. *J. Raman Spectrosc.* **1994**, 25.
(5) Nie, S.; Chu, D. T.; Zare, R. N. *Science* **1994**, *266*, 1018.
(6) Hajatdoost, S.; Olsthoorn, M.; Yarwood, J. In *Proceedings of the XVth International Conference on Raman Spectroscopy*; Asher, S. A., Stein, P., Eds.; J. Wiley: New York, 1996; p 1164.
(7) Stelman, C. M.; Booksh, K. S.; Myrick, M. L. *Appl. Spectrosc.* **1996**, *50*, 552.
(8) Sijtsema, N. M.; Duindam, J. J.; Puppels, G. J.; Otto, C. J. Greve, *J. Appl. Spectrosc.* **1996**, *50*, 545.
(9) Ishidao, T.; Sugimoto, H.; Onoue, Y.; Song, I. S.; Iwai, Y.; Arai, Y. *J. Chem. Eng. Jpn.* **1997**, *30*, 162.
(10) Gehrke, S. H. *Adv. Polym. Sci.* **1993**, *110*, 81.
(11) Asnaghi, D.; Giglio, M.; Bossi, A.; Righetti, P. G. *J. Chem. Phys.* **1995**, *102*, 9736.
(12) Svec F.; Frechet, J. M. J. *Science* **1996**, *273*, 205.
(13) Gross, J. R. United States Patent 5,354,290, 1994.
(14) Li, Y.; Wang, G.; Hu, Z. *Macromolecules* **1995**, *28*, 4194.
(15) Hu, Z.; Chen, Y.; Wang, C.; Zheng, Y.; Li, Y. *Nature* **1998**, *393*, 97.
(16) Hu, Z.; Zhang, X.; Li, Y. *Science* **1995**, *269*, 525.
(17) Matsuo, E. S.; Orkisz, M.; Sun, S. T.; Li, Y.; Tanaka, T. *Macromolecules* **1994**, *27*, 6791.

MA971260C